ACS APPLIED MATERIALS & INTERFACES

Research Article

www.acsami.org

Evaluation of the Catalytic Activity and Cytotoxicity of Palladium Nanocubes: The Role of Oxygen

Eshan Dahal,[†] Jessica Curtiss,[†] Deepak Subedi,[†] Gen Chen,[§] Jessica P. Houston,[§] and Sergei Smirnov*[,†]

[†]Department of Chemistry and Biochemistry, New Mexico State University, Las Cruces, New Mexico 88003, United States

[§]Department of Chemical Engineering, New Mexico State University, Las Cruces, New Mexico 88003, United States

Supporting Information

ABSTRACT: Recently, it has been reported that palladium nanocubes (PdNC) are capable of generating singlet oxygen without photoexcitation simply via chemisorption of molecular oxygen on its surface. Such a trait would make PdNC a highly versatile catalyst suitable in organic synthesis and a Reactive Oxygen Species (ROS) inducing cancer treatment reagent. Here we thoroughly investigated the catalytic activity of PdNC with respect to their ability to produce singlet oxygen and to oxidize 3,3′,5,5′-tetramethylbenzidine (TMB), and analyzed the cytotoxic properties of PdNC on HeLa cells. Our findings showed no evidence of singlet oxygen production by PdNC. The nanocubes' activity is not necessarily linked to activation of oxygen. The oxidation of substrate on PdNC can be a first step, followed by PdNC regeneration with oxygen or other oxidant. The catalytic activity of PdNC toward the oxidation of TMB is very high and shows direct two-electron oxidation when the surface of the PdNC is clean and the ratio of TMB/PdNC is not very high. Sequential one electron oxidation is observed when the pristine quality of PdNC surface is compromised by serum or uncontrolled impurities and/or the ratio of TMB/PdNC is high. Clean PdNC in serum-free media efficiently induce apoptosis of HeLa cells. It is the primary route of cell death and is associated with hyperpolarization of mitochondria, contrary to a common mitochondrial depolarization initiated by ROS. Again, the effects are very sensitive to how well the pristine surface of PdNC is preserved, suggesting that PdNC can be used as an apoptosis inducing agent, but only with appropriate drug delivery system.

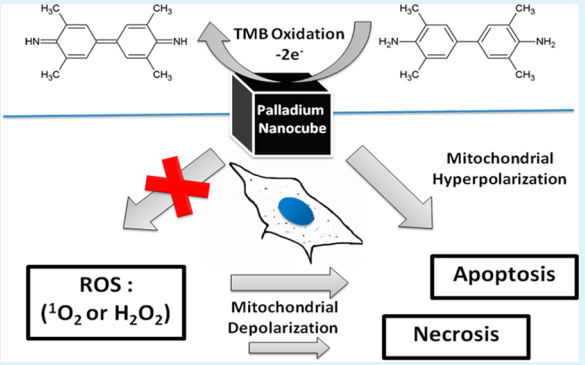

KEYWORDS: *Palladium nanocubes, catalytic activity, cytotoxicity, ROS, cancer treatment*

INTRODUCTION

Singlet oxygen is a highly reactive species that plays an important role in various biologically relevant oxidation processes[1−3] and in cancer therapy.[4−6] However, generating singlet oxygen efficiently is challenging because promoting the triplet ground state of molecular oxygen to a singlet-excited state is a spin-forbidden and energetically demanding process. The lowest energy $^1\Delta_g$ singlet state is ∼1 eV above the ground state. Generally, photosensitizers are used to produce singlet oxygen.[4−56] Recently, metal nanoparticles of different morphology were shown to sensitize formation of singlet oxygen by photoexcitation via their surface plasmon resonance (SPR) bands. Spherical metal nanoparticles such as Au, Ag, and Pt can promote sensitization of singlet oxygen upon exposure to visible light,[7] whereas Au nanorods and decahedral Ag nanoparticles can produce singlet oxygen by near-infrared (NIR) irradiation.[8]

Metallic nanoparticles have shown promising results as versatile catalysts for peroxidation of olefins and photodynamic therapy reagents for cancer treatment.[7−10] Wilkinson et al. showed that spherical palladium nanoparticles could induce apoptosis in human primary bronchial epithelial cells (PBEC), but not in the human alveolar carcinoma cell line (A549).[10] In a recent paper, Long et al.[9] reported that palladium nanocubes (PdNC) were capable of efficiently generating singlet oxygen without any assistance of light, simply via chemisorption of molecular oxygen on their surface. Stronger binding of oxygen to (100) surface of nanocubes apparently had a greater effect than (111) surface of octahedrons. Electron transfer from the Pd(100) surface to the adsorbed molecular oxygen was believed to facilitate the spin-flip process.[9] In the proposed electron transfer mechanism, it was speculated that the decrease in the magnetic moment of chemisorbed O_2 spontaneously enabled the change in the spin state of O_2 from triplet to singlet, despite the higher energy of the latter. Such a peculiar trait, where no photoirradiation is required to form singlet oxygen, if possible, would make PdNC a highly versatile catalyst in organic synthesis and a convenient Reactive Oxygen Species (ROS) inducing cancer treatment reagent. Therefore, in this paper, we first thoroughly investigated the capability of PdNC in producing singlet oxygen and then assessed their catalytic activity toward oxidation of 3,5,3′,5′-tetramethyl-benzidine

Received: August 11, 2014
Accepted: April 17, 2015
Published: April 17, 2015

DOI: 10.1021/am509124x
ACS Appl. Mater. Interfaces 2015, 7, 9364−9371

(TMB) along with the detailed analysis of their cytotoxicity on HeLa cells.

MATERIALS AND METHODS

Synthesis of Palladium Nanocubes (PdNC). PdNC were synthesized following the published protocol, by reducing Pd from K_2PdCl_4 (Sigma-Aldrich) using ascorbic acid in the presence of poly(vinylpyrrolidone) and KBr.[9,11] The size of PdNC was controlled by reaction time and typically was ~10 nm. In a typical synthesis, 105 mg of poly(vinylpyrrolidone) (PVP, Sigma-Aldrich), 300 mg of KBr (Sigma-Aldrich) and 60 mg of ascorbic acid (Sigma-Aldrich) were mixed in 8 mL of deionized water and heated in 50 mL 3-neck flask (with a stir bar, 320 rmp) at 80 °C for 5 min. Subsequently, a solution of 65 mg of K_2PdCl_4 in 3 mL of deionized water was added into the flask. The reaction mixture was heated for 3 h. The resulting product was collected and washed first with acetone, and then consecutively with ethanol and water multiple times, collecting PdNC by centrifugation. Washing multiple times in EtOH and water is crucial and affects the properties of PdNC significantly. Each washing step involved 5 min sonication of 1 mg PdNC suspended in 1 mL of solvent (ethanol or DI water) followed by centrifuging to collect PdNC.

TEM (including high-resolution TEM) images were taken on a JEOL 2010 by dropcasting samples of suspended in water PdNC onto carbon-coated copper grids.

Detection of Singlet Oxygen. Invitrogen's Singlet Oxygen Sensor Green (SOSG) was employed for direct detection of singlet oxygen.[7,8,12] SOSG becomes fluorescent upon oxidation of its anthracene moiety by $^1O_2$*, which makes it very specific for the latter. Twenty-five mg/L of PdNC was added to 5 μM SOSG in D_2O and fluorescence spectra were recorded upon excitation at 480 nm as a function of time using PerkinElmer LS 55 Luminescence Spectrometer.

Oxidation of TMB. In a typical experiment, suspension of PdNC (typically to the final concentration between 10 or 25 mg/L) was added to 2 mL of TMB (3,3′,5,5′-tetramethylbenzidine) solution (typically between 2.5 and 8.9 μM) in acetic buffer solution (HAc/NaAc 1:1, 0.2 M) at 10 °C, and UV−vis absorption spectra (Agilent 8453) of TMB oxidation products were recorded as a function of time. Because the solubility of TMB is fairly small, its solutions were centrifuged to remove the undissolved particles, and the concentration was calculated by absorbance at 285 nm ($\varepsilon = 2.1 \times 10^4$ $M^{-1}cm^{-1}$).[20] In experiments with H_2O_2, the TMB solution was bubbled for 5 min with Ar, again for 5 min after adding PdNC before collecting the spectra, and another 5 min after adding H_2O_2.

In an alternative geometry, either 20 or 200 μg of purified PdNC were immobilized on the surface of a PTFE membrane (Sigma-Aldrich S7062−50EA Cameo Syringe Filter, pore size 0.22 μm, 17 mm diameter) with and without 25 μg of semiconducting single wall carbon nanotubes (SWCNT) with a broad distribution of diameters near ~1.3 nm, from OCSiAl (Tuball). The adhesion of PdNC on PTFE membrane is so strong that withstands even sonication. The adhesion did not compromise when SWCNT were first deposited on the membrane. SEM and TEM images of the PdNC@SWCNT are shown in Supporting Information (SI) Figure S6. Solution of TMB in the acetic buffer with concentration of either 15 μM or 30 μM was passed through the membrane using a syringe pump at a constant rate of 0.1 mL/min. Every 6 min, the collected 0.6 mL of filtrate was used to take a UV−vis spectrum. For experiments in argon, the solution was bubbled in the syringe for 15 min by the corresponding high purity gas prior to measurements.

Cell Culture. Immortalized human epithelial HeLa cells (ATCC, CCL-2) were cultured in T-25 flasks in Dulbecco's modified Eagles Medium (DMEM, Santa Cruz Biotechnology) supplemented with 10% fetal bovine serum. Cells were maintained in the incubator at 37 °C under 5% CO_2 and 95% relative humidity. After reaching 80% confluency, the cells were split using trypsin (0.25%) and reseeded with appropriate seeding density either into a T-25 flask to continue to grow them or in 12 well plates for different cytotoxicity assays. Typically, in 12-well plates, 100 000 of viable HeLa cells were seeded per well in 1 mL of cell culture medium for 24 h prior to experiments.

Mitochondrial Membrane Potential and Cell Viability Assays. Dual staining by rhodamine 123 (Rh 123, Sigma-Aldrich) and propidium iodide (PI, Sigma-Aldrich) was performed on the live HeLa cells treated with either PdNC or hydrogen peroxide. The staining was performed following the published protocol[13] with employing flow cytometry for simultaneous assessment of the mitochondrial membrane potential and late apoptotic/necrotic cells (cell viability). Briefly, PdNC (425 μg/mL) and H_2O_2 (5.6 mM) were incubated separately with HeLa cells in 12-well plates in the cell culture medium with and without serum. Cells without PdNC acted as a negative control, whereas cells with H_2O_2 are considered as a positive control. After 24 h of incubation, cells were trypsinized and suspended (including floating cells) in the 1 mL of cell culture medium with 20 μL of 10 μM Rh123. Following incubation for 20 min at 37 °C, cells were centrifuged at 300*g* for 5 min at room temperature and resuspended in 1 mL PBS. After that, 10 μL of 1 mg/mL PI was added to the resuspended cells and incubated for 5 min at room temperature in the dark. Fluorescence intensity statistics (from 10 000 cells) were immediately analyzed by flow cytometry (BD Accuri C6, Becton Dickinson) with 488 nm laser excitation. Forward scattered light and side scattered light intensities were collected (488 nm), in addition to the fluorescence from Rh123 at 530 ± 30 nm and PI above 600 nm.

DNA Fragmentation Assay. Cells were incubated with PdNC or H_2O_2 as described above in the mitochondrial membrane potential and the cell viability assays. After 24 h of incubation, cells were trypsinized and suspended (including floating cells) in 1 mL of PBS and centrifuged at 200*g* for 5 min at room temperature. The literature protocol for DNA fragmentation assay[14] was exactly followed. Cell pellets were resuspended in 500 mL PBS and fixed with 4.5 mL of 70% (v/v) cold ethanol. Fixed cells were first washed in PBS and then resuspended in 0.5 mL of PBS and 0.5 mL of DNA extraction buffer (192 mL of 0.2 M Na_2HPO_4 with 8 mL of 0.1% Triton X-100). The suspension was kept at room temperature for 5 min and then centrifuged at 400*g* to remove the supernatant. Cells were then resuspended in 1 mL of DNA staining solution (200 μg of PI in 100 mL of PBS plus 20 mg of DNase free RNase) and incubated for 30 min at room temperature in the dark before flow cytometry analysis. 10 000 cells were analyzed by flow cytometry (BD Accuri C6, Becton Dickinson) with 488 nm laser excitation and collection of red fluorescence (>600 nm) as well as forward and side scattered light (488 nm). Cells displaying hypodiploid (sub-G1) DNA content in the cytometry data represent the apoptotic cells.

RESULTS AND DISCUSSION

To thoroughly investigate the capability of PdNC in producing singlet oxygen, we first synthesized high quality PdNC following the procedure of Long et al.,[9] who claimed that PdNC could produce singlet oxygen. PdNC were synthesized by reducing Pd from K_2PdCl_4 using ascorbic acid in the presence of PVP and KBr. Figure 1 shows the TEM and HRTEM images of PdNC resulting from such synthesis. The size of PdNC was controlled by reaction time and was found to be typically around 10 nm. The morphology of PdNC was similar to that published in the literature with the typical 1.9 Å spacing between fringes, characteristic of Pd(200).[9,11] See also SI Figure S2 for details.

The capability of PdNC in producing singlet oxygen without photoirradiation can be directly tested by using Singlet Oxygen Sensor Green (SOSG), a singlet oxygen-specific fluorescent sensor composed of fluorescein and anthracene moieties.[12,15] SOSG becomes strongly fluorescent with an emission maximum at 525 nm upon oxidation of its anthracene moiety by $^1O_2$*.[15] Because of its high sensitivity and specificity toward singlet oxygen,[12] SOSG has been already used in direct detection of singlet oxygen produced by metal nanoparticles[7,8]

DOI: 10.1021/am509124x
ACS Appl. Mater. Interfaces 2015, 7, 9364−9371

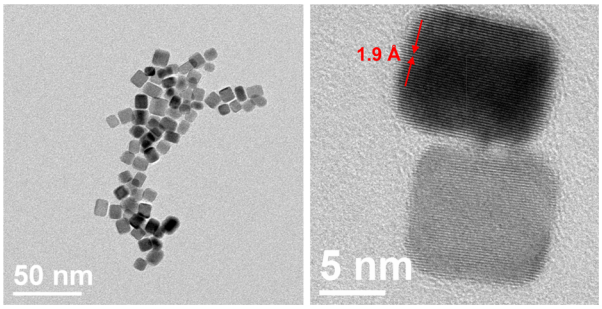

Figure 1. TEM images of PdNC. The high resolution TEM on the right shows the spacing of 0.19 nm between (200) planes. See the SI for details.

and by porous silicon nanoparticles.[16] It has even been used in detection of singlet oxygen inside mammalian cells[17] and in quantitative measurements of singlet oxygen generation.[18] In our experiment, green fluorescence of SOSG in D_2O was recorded upon excitation at 480 nm as a function of time after addition of 25 mg/L PdNC. No increase in fluorescence of SOSG was observed in the time interval from 10 s to 6 h. Figure 2 shows representative fluorescence spectra of SOSG

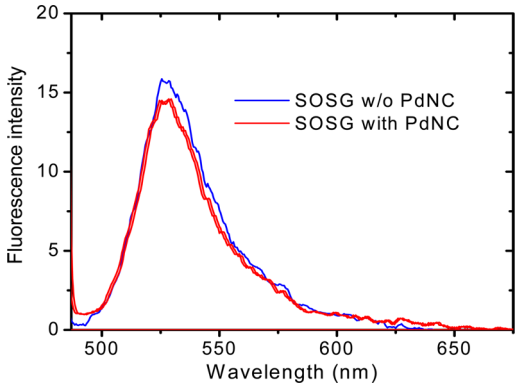

Figure 2. Fluorescence signal of 5 μM SOSG after 10 min with 25 mg/L PdNC (red) and without it (blue). No increase in the fluorescence intensity with PdNC indicates lack of free singlet oxygen production.

before and after adding PdNC. No increase in the fluorescence of SOSG was observed irrespective of bubbling the solution with oxygen and/or increasing the concentration of PdNC. Overall, our findings clearly show no evidence of direct free singlet oxygen production by PdNC.

At the time this paper was under preparation for publication, another report from the same group appeared[19] in which the authors have tried to be more specific and, instead of referring to active molecules as singlet oxygen, they called them "species that behaves like singlet O_2 both chemically and physically".[19] It remains unclear to what that analogy pertains, but now the authors imply that the activated oxygen molecules do not leave the surface of PdNC until the reaction with the substrate. Thus, the catalytic activity of PdNC cannot be simply reduced to activation of oxygen and needs to be evaluated for oxidation of a substrate.

One of the convenient substrates reported in ref 9, 3,3′,5,5′-tetramethylbenzidine (TMB), can be used for evaluating the catalytic activity of PdNC in more details. TMB is often used in spectrophotometric[20] and electrochemical[21−23] immunosorbent assays. It can be oxidized electrochemically[21−23] or by a strong oxidant, such as hydrogen peroxide[19,24] or oxygen[9] but typically needs a catalyst to achieve a reasonable rate. The oxidation products can be easily distinguished (see Scheme 1): the one-electron oxidation intermediate TMB^+ gives a blue color due to charge transfer absorption peaks at 370 and 652 nm, while the two-electron oxidation final product diimine TMB^{2+} has the absorption peak at 450 nm.[20]

UV−vis spectra of TMB solutions at different times after adding PdNC are shown in Figure 3. The spectroscopic changes are not exactly the same as in ref 9. Notably, Figure 3A illustrates that TMB can be oxidized directly into two-electron oxidation final product TMB^{2+} immediately from the beginning of the reaction. It bypasses the one-electron oxidation intermediate TMB^+ (reaction pathway "a" in Scheme 1) or, at least, passes very quickly through it. Sequential oxidation of TMB (reaction pathway "b" in Scheme 1) reported by Long et al. and attributed to oxidation by singlet oxygen or its analogue[9] is observed when PdNC are insufficiently clean and/or the relative amount of TMB is too high. In Figure 3B such a situation is illustrated for the same concentrations of PdNC and TMB as in Figure 3A but with insufficiently cleaned PdNC. Washing PdNC after synthesis with ethanol and water multiple times and using them fresh is vital to observation of direct two-electron oxidation. As a matter of fact, the suggested protocol of washing 3 times in ethanol[9] is insufficient to achieve "pristine" quality PdNC. FTIR analysis indicates residual hydrocarbon CH bonds even after additional 5 washings in water. By the ninth washing in water, almost no residual methylene bands were observed (SI Figure S1). Note that singlet oxygen production was not detected for either "poorly cleaned" PdNC or for the highest quality of purification. When the PdNC surface is insufficiently clean or is compromised by serum or uncontrolled impurities after long storage, sequential one electron oxidation as in Figure 3B is observed. In this case, both, the intermediate TMB^+ and the final TMB^{2+} oxidized products appear immediately after adding PdNC but majority of the TMB molecules eventually converts into TMB^{2+} gradually with time (see also SI Figure S3).

The catalytic role of PdNC, as of any other catalyst in a redox reaction, can be crudely divided into two options: activation (oxidation) of a reductant, TMB in this case, or activation (reduction) of an oxidant. The latter can be oxygen, hydrogen peroxide, or other reagents with sufficient reduction potential. In the assay for H_2O_2 with horseradish peroxidase (HRP) and TMB, it has been shown that the initial reaction of peroxide with HRP is followed by formation of TMB^+.[24] The case of PdNC catalyzed oxidation of TMB or other substrates does not have to be the same. Opposite to Long et al.[9,19] who believe that it originates exclusively by oxygen activation to produce "singlet oxygen like species", we suggest considering both routes and believe that direct oxidation of a substrate by PdNC is likely to happen as well and, in some cases like with TMB, can be just as important if not more. Oxygen is a very strong oxidant with the redox potential sufficient for oxidizing TMB to TMB^{2+} while H_2O_2 seizes at the first step, i.e., production of TMB^+. Nevertheless, PdNC catalyzes both reactions; as seen in SI Figure S5 for H_2O_2. Oxidation of TMB by hydrogen peroxide can be also achieved with other metal or metal oxide nanoparticles,[25−28] as well as electrochemically.[21−23] All these suggest that PdNC activated O_2 is not unique in oxidizing TMB, and it does not have to be exclusively via oxygen activation.

DOI: 10.1021/am509124x
ACS Appl. Mater. Interfaces 2015, 7, 9364−9371

Scheme 1. Reaction Pathways for Oxidation of TMB, Partially Adopted from Ref 20[a]

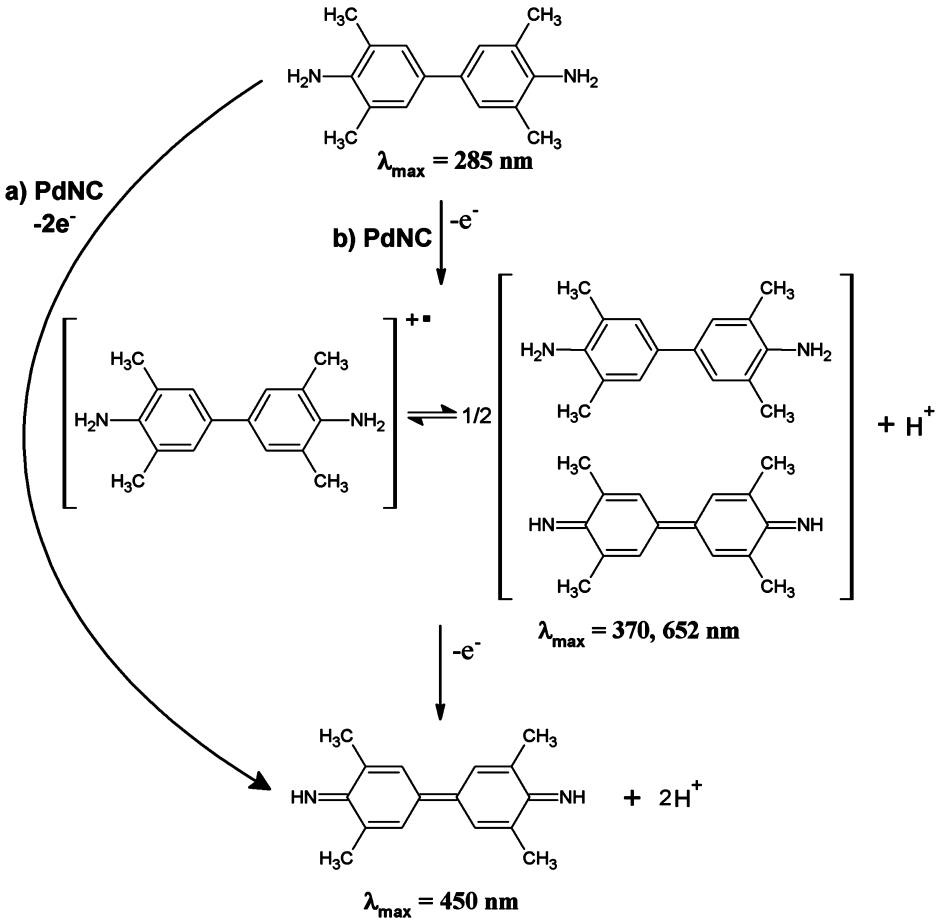

[a]Pathway a) represents the oxidation of TMB into direct two-electron oxidation final product, and pathway b) represents sequential one electron oxidation of TMB.

There are other indications of a possibility that this reaction can start with direct oxidation of TMB on the surface of PdNC. One notices that the absorption peak of TMB monomer at 285 nm gets strongly suppressed upon addition of PdNC before any oxidation products are observed. It correlates with the previously reported higher binding affinity of TMB^{2+} on metal surfaces in electrochemical oxidation of TMB.[23] Optical absorption of TMB (or its oxidized forms) on the metal surface is significantly suppressed as it is well-known for molecules strongly coupled to a metal surface with the transition moment parallel to it.[29,30]

One can speculate that PdNC is a strong enough oxidizer to oxidize TMB to TMB^{2+} on its surface similar to electrochemical oxidation easily seen for TMB at high enough potential.[21−23] Because PdNC is not kept at a constant potential, its Fermi energy shifts upon accepting electrons and eventually making PdNC incapable to oxidize further. The overall oxidative capacitance of PdNC (the maximum amount of stored negative charge) is limited by the PdNC concentration and presence of oxygen or other oxidant in the solution that helps to recuperate their catalytic activity. Indeed, oxidation of TMB does not completely cease in Ar, in Figure 1C of ref 9 it only slowed down. In SI Figure S5, under similar conditions, it shows suppression of TMB^{2+} production but one electron oxidation to TMB^{+} is still present. Long et al. also had demonstrated[19] the importance of the charge state on the PdNC surface and were able to enhance the oxidation yields by photoinduced charge injection from TiO_2 in the corresponding PdNC/TiO_2 hybrid. Unfortunately, they did not confirm the unique role of oxygen by using oxygen free conditions. Since other oxidizers, such as hydrogen peroxide, also can oxidize TMB with catalytic "help" (see SI Figure S5), i.e., by capturing charge from PdNC ("reoxidizing" it), the role of oxygen does not appear unique and can be replaced.

One can extend the idea of charge injection or controlling the Fermi energy without photoexcitation. To this goal, we have conducted experiments with the high purity PdNC bound to the surface of a PTFE membrane while solution of TMB is pushed through at a constant rate (0.1 mL/min). In this pseudo continuous approach, we can manipulate separately with the states of PdNC and TMB in solution while measuring the kinetics of the reaction by collecting products in the filtrate solution for analysis of small aliquots (0.6 mL). Figure 4 illustrates the results for the two conditions of high (A−C) and low (D−F) ratios between the PdNC and TMB amounts: 200 μg PdNC/15 μM TMB (A−C) and 20 μg PdNC/30 μM TMB (D−F). The kinetic behaviors observed in air and in Ar are dramatically different and depend on the PdNC/TMB ratio. First of all, lowering the ratio causes almost disappearance of the TMB^{2+} peak at 450 nm and leads to significant survival of unoxidized TMB at 285 nm, as seen in comparing Figure 4, parts A and D. At low PdNC/TMB ratios, the unoxidized TMB comes off at an amount slightly smaller than that in the original solution only at the beginning. At higher PdNC/TMB ratios,

DOI: 10.1021/am509124x
ACS Appl. Mater. Interfaces 2015, 7, 9364−9371

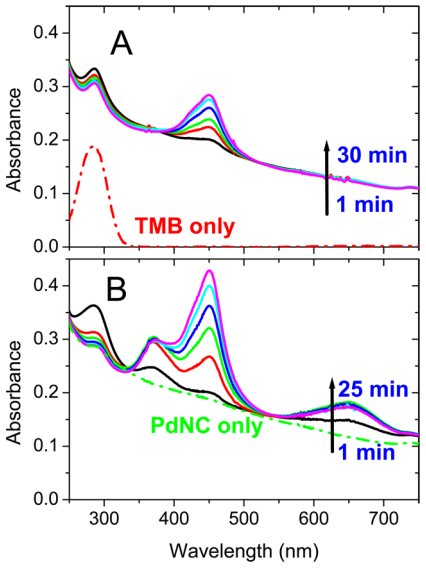

Figure 3. Time dependent UV−vis spectra of TMB solutions upon addition of PdNC: a) with PdNC washed more than 20 times in ethanol and water and b) with PdNC washed five times in ethanol and water. The 0 min curve in the latter corresponds to PdNC only. Concentration of PdNC used was ∼25 mg/L and [TMB] concentration 8.9 μM. The absorbance peaks for one-electron oxidation intermediate are seen at 370 and 652 nm and the absorption peak for the two electron-oxidation final diimine product is seen at 450 nm.

almost no unoxidized TMB comes through at first. Its amount builds up very slowly and does not reach even 20% of the original amount in solution within the course of 30 min. At the same time, the amount of product significantly increases with time (Figure 4A), similar to that in SI Figure S3. The TMB^{2+} is favored at first, but gradually gives way to the one electron oxidized products. As shown in Figure 4B, deoxygenating the solution by bubbling with argon instantaneously releases unoxidized TMB (data for Figure 4B were collected in the same run right after part A) and suppresses production of the TMB^{2+} diimine. The latter is not surprising because the oxidation potential of TMB increases between the one- and two-electron products and thus production of TMB^{2+} should cease first. The effect of an "oxygen free" atmosphere is particularly pronounced for the low PdNC/TMB ratio (Figure 4E), where not only production of TMB^{2+} is suppressed, but also the yield of TMB^{+} declines with time as well. All of these can be rationalized by PdNC being a rate limiting component that has a finite oxidizing (charge) capacity and oxygen needing only to reoxidize PdNC. From the total amount of oxidized product in the latter case, one can approximate that each PdNC performed on the order of $\sim 3 \times 10^3$ oxidations in Ar (see SI), which is the upper limit estimate because some residual oxygen might be still present in the solution due to its traces in Ar and imperfections in the procedure. A crude estimate based on the double layer capacitance gives the maximum turnover number for each PdNC without reoxidation $\sim 10^3$, which is not such a dramatic discrepancy given the above-mentioned possibility of oxygen traces (see SI).

Regeneration of PdNC can be achieved by other means, for example by hydrogen peroxide or by carbon nanotubes (CNT), instead of oxygen. SWCNT are more convenient for our experiment with membrane. The Fermi energy of SWCNT depends on their diameter and doping[31] but is typically higher than that of Pd. For small diameter *p*-doped SWCNT the difference in Fermi levels becomes quite small so that one can anticipate insignificant charge transfer from SWCNT to Pd and,

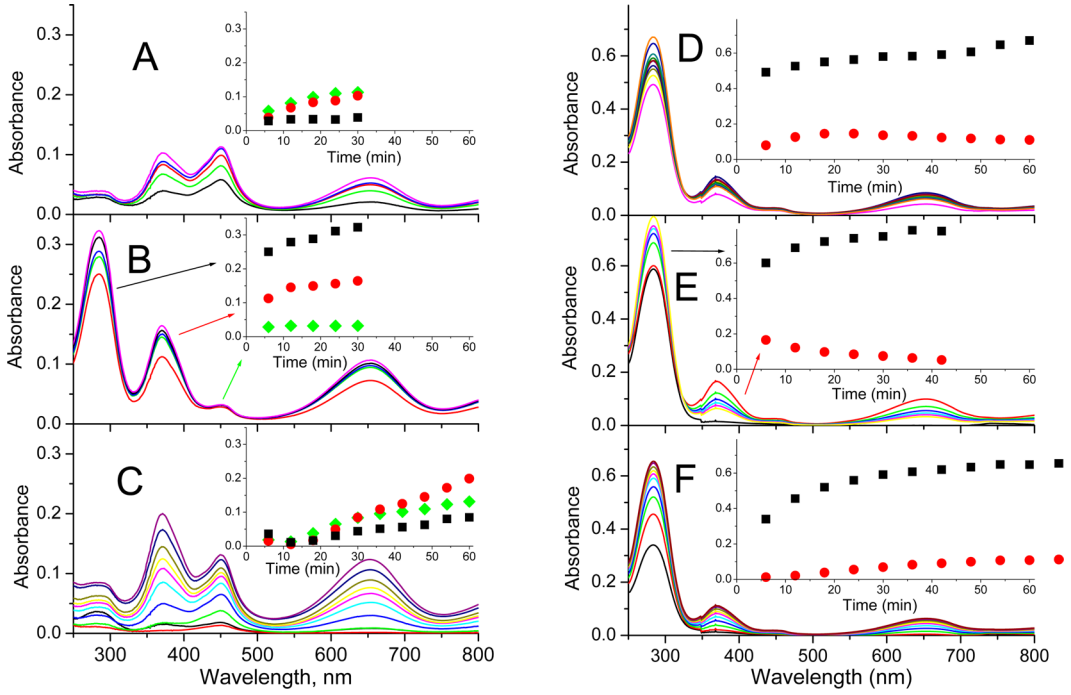

Figure 4. Kinetics of TMB oxidation (concentrations 15 μM in (A−C) and 30 μM in (D−F)) in the pseudo continuous geometry with PdNC immobilized on filter membrane at the amount of 200 μg (A−C) and 20 μg (D−F). A and D are in air; B and E, argon; while C and F are in argon but PdNC were also supported by 25 μg of SWCNT. The insets show time-evolution of the absorbance for unoxidized TMB (285 nm, black squares), single-electron oxidized (370 nm, red circles) and two-electron oxidized (450 nm, green rhombs) TMB peaks. See text for details.

DOI: 10.1021/am509124x
ACS Appl. Mater. Interfaces 2015, 7, 9364−9371

at the same time, sufficient to oxidize TMB at least to TMB^{+}.[31] There is a significant distribution of redox potentials for SWCNT even of the same diameter,[32] which ensures that there is noticeable population of SWCNT with redox potentials capable to support TMB oxidation to TMB^{2+}.

We placed the same amounts of PdNC (20 μg and 200 μg) on the surface of single walled CNT (SWCNT). Even though the amount of SWCNT was only 25 μg, its addition significantly increased the charge capacitance and allowed charge collection from PdNC, even when the amount of TMB was quite high (Figure 4C). Note that for PdNC@SWCNT in Ar, the TMB^{2+} product is clearly visible at 450 nm. Although, the kinetics of TMB oxidation with PdNC@SWCNT in Ar is different from that for PdNC in air (compare Figure 4, parts A with C and D with F, respectively) primarily due to capturing of TMB directly on SWCNT. Notably, SWCNT without PdNC do not oxidize TMB at all (SI Figure S7), while elution of TMB is clearly delayed due to capturing of TMB on SWCNT.

The suggested mechanism of PdNC catalytic activity bypassing the oxygen involvement cannot be uniformly applied, especially for reactions where oxygen ends up in the product, but we believe that the situation with TMB is not unique. In any case, we see no indication of free ROS that get produced by PdNC. Besides, as we saw above, hydrogen peroxide gets reduced on PdNC via oxidation of TMB and thus is also unlikely produced by PdNC in ambient conditions. The issue of the mechanism of oxidation with PdNCs becomes particularly important when it comes to their possible medical applications. The remaining part of the study deals with evaluation of the effects of PdNCs in cancer treatment, in particular, the detailed analysis of their cytotoxic properties on HeLa cells.

It was previously shown through MTT assay that PdNCs significantly reduced the viability of HeLa cells.[9] So far, the mechanism of cytotoxicity induced by PdNCs is not well understood and requires further study. Herein we offer some insight by differentiating apoptosis and necrosis in the PdNC treated HeLa cells and by analyzing the change in the mitochondrial membrane potential in them.

DNA fragmentation is an established marker of apoptosis.[14] We performed DNA fragmentation assay with flow cytometry to verify whether PdNC induces apoptosis in HeLa cells. As shown in Figure 5 (see also SI Figure S8 for details), 425 μg/mL of PdNCs induce DNA fragmentation in HeLa cells associated with apoptosis, but most effectively in the serum free cell culture media. There is a roughly 3.5-fold increase in the number of apoptotic cells after treatment with PdNC in the absence of serum. Cells treated with 5.6 mM of H_2O_2 (positive control) also effectively induced apoptosis in the serum free media, whereas untreated cells (negative control) showed no significant increase in apoptotic behavior without serum. The effect of serum on compromising the efficacy of PdNC to induce apoptosis is likely of two causes. On one hand, different proteins, antibodies, and antigens present in serum can "heal" the cytotoxic effect, similar to that in the case of H_2O_2.[33] On the other hand, these serum components can also wrap around PdNC to coat them and thus decrease their surface activity. Formation of a protein corona around nanoparticles in a biological milieu is well-known.[34] It suggests that PdNC can be used as an apoptosis-inducing agent, but only with an appropriate drug delivery system that preserves its pristine surface before contact with the cancer cells.

The apoptotic mechanism of PdNC cytotoxicity confirmed by the DNA fragmentation assay does not clarify whether it is the same or different from the effect of hydrogen peroxide or other reactive oxygen species (ROS). Additional information is required to elucidate the mechanism of the PdNC cytotoxicity effect. The mitochondrial membrane potential has been extensively used in studies of such phenomena.[35,36] Mitochondria play an important role in mediating apoptosis in most of the apoptotic pathways.[37] In particular, reactive oxygen species, like singlet oxygen and hydrogen peroxide, damage mitochondria and induce the loss of the mitochondria membrane potential in the process of triggering apoptosis.[38−41] This collapse of mitochondrial potential, an early sign of mitochondrial-mediated apoptosis, can be tracked using Rhodamine 123 (Rh123). Rh123 is a mitochondria specific cationic fluorescent dye commonly used to assess mitochondrial membrane potential.[13,35,36] The uptake of Rh123 in mitochondria is directly proportional to the mitochondrial membrane potential.[36] We employed this technique to further investigate the mechanism of PdNC induced apoptosis.

As seen in Figure 6 (see also SI Figure S9 for details), HeLa cells treated with H_2O_2 (positive control) show a decrease in the fluorescence intensity of Rh123 as compared to the untreated cells. As expected from literature,[38−41] ROS like

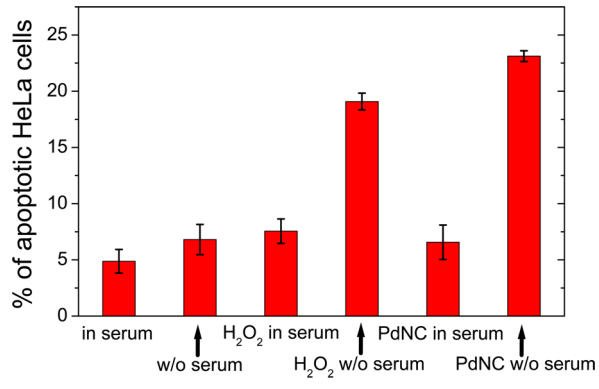

Figure 5. Percent of the apoptotic HeLa cells after treatment with PdNC and H_2O_2 in the cell culture medium with and without serum measured as the mean percentage of cells displaying hypodiploid (sub-G1) DNA content using flow cytomeric analyses. Data represents the mean for two independent experiments.

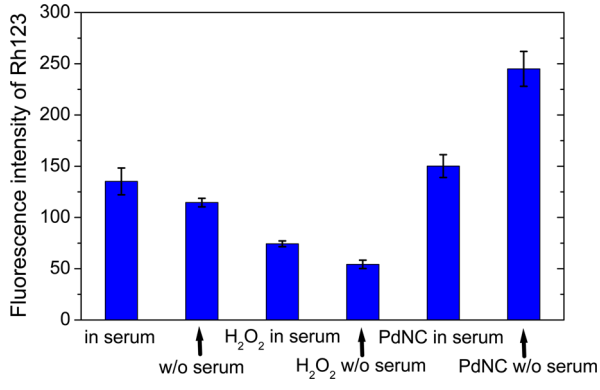

Figure 6. Analysis of the mitochondrial membrane potential by Rh123 uptake in HeLa cells treated with PdNC and H_2O_2 in the cell culture medium with and without serum. Data represent the mean of fluorescence intensity of cells analyzed using flow cytometry from three independent experiments.

DOI: 10.1021/am509124x
ACS Appl. Mater. Interfaces 2015, 7, 9364−9371

H_2O_2 depolarized the mitochondria (decrease of the mitochondria membrane potential). However, HeLa cells treated with PdNC showed the opposite effect—hyperpolarization of the mitochondria membrane potential (see also the confocal images in SI Figure S11). Such a behavior is not uncommon; mitochondrial membrane potential in HeLa cells can be increased by treating with manganese(II)[42] or nigericin,[43] but it is quite opposite to typical effects of various ROS. Note that, again, the increase in the mitochondrial membrane potential is more pronounced when the cells were treated with PdNC in the cell culture medium without serum, while depolarization by H_2O_2 was also more pronounced without serum. The effect of serum is in alignment with the DNA fragmentation, but with opposite signs for hydrogen peroxide and PdNC.

PI staining can be used for discriminating cells undergoing late apoptosis or necrosis (nonviable cells). PI can only permeate into nonviable cells because of their compromised plasma membrane integrity.[13] Figure 7 shows that only 6.6% with serum and 14.7% without serum of cells treated with 425 μg/mL of PdNC were nonviable (see also SI Figure S9 for details), which is slightly less than the number of apoptotic cells from DNA fragmentation assay (Figure 5). The effect of hydrogen peroxide is clearly different—the number of nonviable cells was greater than the apoptotic cells: 40.9% with serum and 46.3% without serum. Untreated cells (negative control) showed no significant amount of nonviable cells, which was also smaller than the number of apoptotic cells. The lower yield of nonviable cells for PdNC treatment in serum again emphasizes the effectiveness of PdNC in the serum free biological environment. The dramatic difference for hydrogen peroxide treatment, where the amount of nonviable cells significantly exceeds that of the apoptotic cells, suggests that the necrotic pathway is dominant in that case. PdNC treatment, however, with 23% of apoptotic cells from DNA fragmentation assay being much greater than 14.7% of total nonviable cells, indicates that necrosis is a minor route of cell death induced by PdNC. It also implies that PdNC do not produce hydrogen peroxide or singlet oxygen as cytotoxic ROS. Thus, the mechanism of PdNC toxicity is different from ROS, mainly induces apoptosis, at least in HeLa cells, and is accompanied by hyperpolarization of mitochondrial membrane potential.

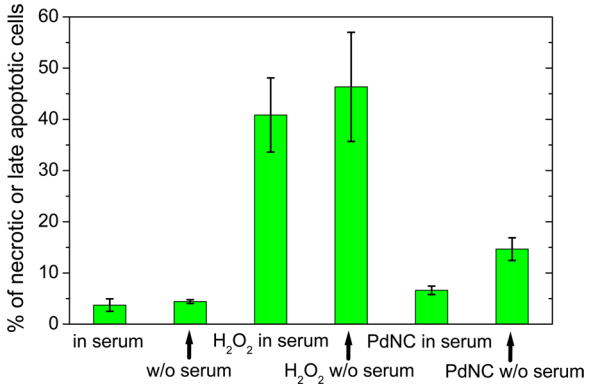

Figure 7. Percent of nonviable cells (necrotic or late apoptotic) by PI uptake in the HeLa cells treated with PdNC and H_2O_2 in the cell culture medium with and without serum. Data represent the mean fluorescence intensity of PI coming from cells analyzed using flow cytometery from three independent experiments.

CONCLUSIONS

In conclusion, Pd nanocubes provide efficient catalytic surfaces for oxidation of multiple substrates but do not produce singlet oxygen, as previously reported.[9] Nevertheless, direct two-electron oxidation of TMB is observed when surface of PdNC is clean and the ratio of TMB/PdNC is not very high, which indicates a strong oxidative ability of PdNC and sensitivity to surface fouling. The nanocubes' activity is not necessarily linked to oxygen, which only serves as a reoxidant of PdNC, at least in oxidizing TMB, and can be alternatively substituted by SWCNT. PdNC also efficiently induce apoptosis of HeLa cells but by a mechanism different from that of ROS and associated with hyperpolarization of mitochondria. The effects are very sensitive to how well the pristine surface of PdNC is preserved, suggesting that PdNC can be used as an apoptosis inducing agent, but only with the appropriate drug delivery system.

ASSOCIATED CONTENT

Supporting Information

FTIR of PdNC at different stages of cleaning, detailed analysis of HRTEM, additional kinetics of TMB oxidation, detailed flow cytometry data for DNA fragmentation and mitochondrial membrane potential assays, confocal microscopy images, SEM and TEM of PdNC@SWCNT, and estimation of the oxidation turnover number for PdNC. The Supporting Information is available free of charge on the ACS Publications website at DOI: 10.1021/am509124x.

AUTHOR INFORMATION

Corresponding Author

*Tel: 575-646-1547; Fax: 575-646-2649; E-mail: snsm@nmsu.edu.

Notes

The authors declare no competing financial interest.

ACKNOWLEDGMENTS

This work was partially supported by a grant from the National Institute of Health (R15-EB-016401-01). The authors are grateful to Dr. P. Cook for help with the TEM and Dr. E. Yukl, Dr. K. Houston, Dr. I. Vlassiouk, and Dr. M. Johnson for helpful discussions.

REFERENCES

(1) Clennan, E. L. New Mechanistic and Synthetic Aspects of Singlet Oxygen Chemistry. *Tetrahedron* **2000**, *56*, 9151–9179.

(2) Corey, E. J.; Taylor, W. C. Study of Peroxidation of Organic Compounds by Externally Generated Singlet Oxygen Molecules. *J. Am. Chem. Soc.* **1964**, *86*, 3881–3882.

(3) Jiang, G.; Chen, J.; Huang, J.-S.; Che, C.-M. Highly Efficient Oxidation of Amines to Imines by Singlet Oxygen and Its Application in Ugi-Type Reactions. *Org. Lett.* **2009**, *11*, 4568–4571.

(4) Ogilby, P. R. Singlet Oxygen: There is Indeed Something New under the Sun. *Chem. Soc. Rev.* **2010**, *39*, 3181.

(5) Triesscheijn, M.; Baas, P.; Schellens, J. H. M.; Stewart, F. A. Photodynamic Therapy in Oncology. *Oncologist* **2006**, *11*, 1034–1044.

(6) DeRosa, M. C.; Crutchley, R. J. Photosensitized Singlet Oxygen and its Applications. *Coord. Chem. Rev.* **2002**, *233*, 351–371.

(7) Vankayala, R.; Sagadevan, A.; Vijayaraghavan, P.; Kuo, C.-L.; Hwang, K. C. Metal Nanoparticles Sensitize the Formation of Singlet Oxygen. *Angew. Chem,. Int. Ed.* **2011**, *50*, 10640–10644.

(8) Vankayala, R.; Kuo, C.-L.; Sagadevan, A.; Chen, P.-H.; Chiang, C.-S.; Hwang, K. C. Morphology Dependent Photosensitization and Formation of Singlet Oxygen ($^1\Delta_g$) by Gold and Silver Nanoparticles

DOI: 10.1021/am509124x
ACS Appl. Mater. Interfaces 2015, 7, 9364–9371

and its Application in Cancer Treatment. *J. Mater. Chem. B* **2013**, *1*, 4379.
(9) Long, R.; Mao, K.; Ye, X.; Yan, W.; Huang, Y.; Wang, J.; Fu, Y.; Wang, X.; Wu, X.; Xie, Y.; Xiong, Y. Surface Facet of Palladium Nanocrystals: A Key Parameter to the Activation of Molecular Oxygen for Organic Catalysis and Cancer Treatment. *J. Am. Chem. Soc.* **2013**, *135*, 3200−3207.
(10) Wilkinson, K. E.; Palmberg, L.; Witasp, E.; Kupczyk, M.; Feliu, N.; Gerde, P.; Seisenbaeva, G. A.; Fadeel, B.; Dahlén, S.-E.; Kessler, V. G. Solution-Engineered Palladium Nanoparticles: Model for Health Effect Studies of Automotive Particulate Pollution. *ACS Nano* **2011**, *5*, 5312−5324.
(11) Li, B.; Long, R.; Zhong, X.; Bai, Y.; Zhu, Z.; Zhang, X.; Zhi, M.; He, J.; Wang, C.; Li, Z.-Y.; Xiong, Y. Investigation of Size-Dependent Plasmonic and Catalytic Properties of Metallic Nanocrystals Enabled by Size Control with HCl Oxidative Etching. *Small* **2012**, *8*, 1710−1716.
(12) Molecular Probe product information, 2004.
(13) Pozarowski, P.; Grabarek, J.; Darzynkiewicz, Z. Flow Cytometry of Apoptosis. *Curr. Protoc. Cell Biol.* **2004**, 18.8.1−18.8.33.
(14) Riccardi, C.; Nicoletti, I. Analysis of Apoptosis by Propidium Iodide Staining and Flow Cytometry. *Nat. Protoc.* **2006**, *1*, 1458−1461.
(15) Kim, S.; Fujitsuka, M.; Majima, T. Photochemistry of Singlet Oxygen Sensor Green. *J. Phys. Chem. B* **2013**, *117*, 13985−13992.
(16) Xiao, L.; Gu, L.; Howell, S. B.; Sailor, M. J. Porous Silicon Nanoparticle Photosensitizers for Singlet Oxygen and Their Phototoxicity Against Cancer Cells. *ACS Nano* **2011**, *5*, 3651−3659.
(17) Gollmer, A.; Arnbjerg, J.; Blaikie, F.; Pedersen, B.; Breitenbach, T.; Daasbjerg, K.; Glasius, M.; Ogilby, P. Singlet Oxygen Sensor Green: Photochemical Behavior in Solution and in a Mammalian Cell. *Photochem. Photobiol.* **2011**, *87*, 671−679.
(18) Lin, H. Y.; Shen, Y.; Chen, D. F.; Lin, L. S.; Wilson, B. C.; Li, B. H.; Xie, S. S. Feasibility Study on Quantitative Measurements of Singlet Oxygen Generation Using Singlet Oxygen Sensor Green. *J. Fluoresc.* **2013**, *23*, 41−47.
(19) Long, R.; Mao, K.; Gong, M.; Zhou, S.; Hu, J.; Zhi, M.; You, Y.; Bai, S.; Jiang, J.; Zhang, Q.; Wu, X.; Xiong, Y. Tunable Oxygen Activation for Catalytic Organic Oxidation: Schottky Junction Versus Plasmonic Effects. *Angew. Chem., Int. Ed. Engl.* **2014**, *53*, 3205−3209.
(20) Josephy, P. D.; Eling, T.; Mason, R. P. The Horseradish Peroxidase Catalyzed Oxidation of 3,5,3′,5′-Tetramethylbenzidine. Free Radical and Charge-Transfer Complex Intermediates. *J. Biol. Chem.* **1982**, *257*, 3669−3675.
(21) Volpe, G.; Compagnone, D.; Draisci, R.; Palleshi, G. 3,3′,5,5′-Tetramethylbenzidine as Electrochemical Substrate for Horseradish Peroxidase Based Enzyme Immunoassays. A comparative study. *Analyst* **1998**, *123*, 1303−1307.
(22) Kui, J.; Tao, Y.; Shuyan, N. A Thin-layer Spectroelectrochemical Study of 3,3′,5,5′- Tetramethylbenzidine at SnO_2:F Film Optically Transparent Electrode. *Sci. China Ser. B* **2004**, *47*, 267−275.
(23) Liu, M.; Zhang, Y.; Chen, Y.; Xie, Q.; Yao, S. EQCM and in situ FTIR Spectroelectrochemistry Study on the Electrochemical Oxidation of TMB and the Effect of Large-Sized Anions. *J. Electroanal. Chem.* **2008**, *622*, 184−192.
(24) Marquez, L. A.; Dunford, H. B. Mechanism of the Oxidation of 3,5,3′,5′-Tetramethylbenzidine by Myeloperoxidase Determined by Transient- and Steady-State Kinetics. *Biochemistry* **1997**, *36*, 9349−9355.
(25) Liu, Y.; Wang, C.; Cai, N.; Long, S.; Yu, F. Negatively Charged Gold Nanoparticles as an Intrinsic Peroxidase Mimic and Their Applications in the Oxidation of Dopamine. *J. Mater. Sci.* **2014**, *49*, 7143−7150; **1997**, *36*, 9349−9355.
(26) He, W.; Wu, X.; Liu, J.; Hu, X.; Zhang, K.; Hou, S.; Zhou, W.; Xie, S. Design of AgM Bimetallic Alloy Nanostructures (M = Au, Pd, Pt) with Tunable Morphology and Peroxidase-Like Activity. *Chem. Mater.* **2010**, *22*, 2988−2994.
(27) Woo, M.-A.; Kim, M. I.; Jung, J. H.; Park, K. S.; Seo, T. S.; Park, H. G. A Novel Colorimetric Immunoassay Utilizing the Peroxidase Mimicking Activity of Magnetic Nanoparticles. *Int. J. Mol. Sci.* **2013**, *14*, 9999−10014.
(28) Asati, A.; Santra, S.; Kaittanis, C.; Nath, S.; Perez, J. M. Oxidase Activity of Polymer-Coated Cerium Oxide Nanoparticles. *Angew. Chem., Int. Ed.* **2009**, *48*, 2308−2312.
(29) Barnes, W. L. Fluorescence Near Interfaces: the Role of Photonic Mode Density. *J. Mod. Optics* **1998**, *45*, 661−699.
(30) Chance, R. R.; Prock, A.; Silbey, R. Molecular Fluorescence and Energy Transfer Near Interfaces. *Adv. Chem. Phys.* **1978**, *37*, 1.
(31) Hirana, Y.; Juhasz, G.; Miyauchi, Y.; Mouri, S.; Matsuda, K.; Nakashima, N. Empirical Prediction of Electronic Potentials of Single-Walled Carbon Nanotubes With a Specific Chirality (n,m). *Sci. Rep.* **2013**, *3*, 2959−5.
(32) Schafer, S.; Cogan, N. M. B.; Krauss, T. D. Spectroscopic Investigation of Electrochemically Charged Individual (6,5) Single-Walled Carbon Nanotubes. *Nano Lett.* **2014**, *14*, 3138−3144.
(33) Kameshwar-Rao, A. S.; Gil, S.; Richter-Landsberg, C.; Givol, D.; Yavin, E. H_2O_2-Induced Apoptotic Death in Serum-Deprived Cultures of Oligodendroglia Origin is Linked to Cell Differentiation. *J. Neurosci. Res.* **1999**, *56*, 447−456.
(34) Monopoli, M. P.; Aberg, C.; Salvati, A.; Dawson, K. A. Biomolecular Coronas Provide the Biological Identity of Nanosized Materials. *Nat. Nanotechnol.* **2012**, *7*, 779−786.
(35) Chen, L. B. Mitochondrial Membrane Potential in Living Cells. *Annu. Rev. Cell Biol.* **1988**, *4*, 155−181.
(36) Ferlini, C.; Scambia, G. Assay for Apoptosis Using the Mitochondrial Probes, Rhodamine123 and 10-N-nonyl Acridine Orange. *Nat. Protoc.* **2007**, *2*, 3111−3114.
(37) Fiers, W. W.; Beyaert, R. R.; Declercq, W. W.; Vandenabeele, P. P. More than One Way to Die: Apoptosis, Necrosis and Reactive Oxygen Damage. *Oncogene* **1999**, *18*, 7719−7730.
(38) Zhuang, S. p38 Mitogen-Activated Protein Kinase Mediates Bid Cleavage, Mitochondrial Dysfunction, and Caspase-3 Activation During Apoptosis Induced by Singlet Oxygen but Not by Hydrogen Peroxide. *J. Biol. Chem.* **2000**, *275*, 25939−25948.
(39) Petrat, F.; Pindiur, S.; Kirsch, M.; de Groot, H. NAD(P)H, a Primary Target of $^1O_2$ in Mitochondria of Intact Cells. *J. Biol. Chem.* **2003**, *278*, 3298−3307.
(40) Brady, N. R.; Elmore, S. P.; van Beek, J. J. H. G. M.; Krab, K.; Courtoy, P. J.; Hue, L.; Westerhoff, H. V. Coordinated Behavior of Mitochondria in Both Space and Time: A Reactive Oxygen Species-Activated Wave of Mitochondrial Depolarization. *Biophys. J.* **2004**, *87*, 2022−2034.
(41) Zamzami, N.; Susin, S. A.; Marchetti, P.; Hirsch, T.; Gómez-Monterrey, I.; Castedo, M.; Kroemer, G. Mitochondrial Control of Nuclear Apoptosis. *J. Exp. Med.* **1996**, *183*, 1533−1544.
(42) Oubrahim, H.; Stadtman, E. R.; Chock, P. B. Mitochondria Play no Roles in Mn(II)-Induced Apoptosis in HeLa Cells. *Proc. Natl. Acad. Sci. U.S.A.* **2001**, *98*, 9505−9510.
(43) Akhmedov, D.; Braun, M.; Mataki, C.; Park, K. S.; Pozzan, T.; Schoonjans, K.; Rorsman, P.; Wollheim, C. B.; Wiederkehr, A. Mitochondrial Matrix pH Controls Oxidative Phosphorylation and Metabolism-Secretion Coupling in INS-1E Clonal Cells. *FASEB J.* **2010**, *24*, 4613−4626.

DOI: 10.1021/am509124x
ACS Appl. Mater. Interfaces 2015, 7, 9364−9371